Wavelet analysis and consensus algorithm-based fault-tolerant control for smart grids

Yunlong Han*

Department of Basic and General Knowledge, Shenyang Institute of Science and Technology, Shenyang, China

In this paper, the voltage and frequency regulation problems are investigated for smart grids under the influence of faults. To solve those problem, a wavelet analysis and consensus algorithm-based fault-tolerant control scheme is proposed. Specifically, the wavelet analysis technique is introduced to determine whether there exist faults or not in the smart grids. Then, a distributed fault estimator is designed to estimate the attack signals. Based on this estimator state, a distributed fault-tolerant controller is designed to compensate for the faults. It is theoretically shown that the developed method can achieve the voltage regulation and frequency objectives. Finally, a smart grid with four distributed generations is constructed in MATLAB/Simulink for simulation to validate the effectiveness.

KEYWORDS

secondary control, fault-tolerant control, voltage regulation, distributed control, AC micro grid

1 Introduction

During the past decades, microgrid (MG) has attracted much attention because of their reliability, efficiency, and so on. AC MG consists of various distributed generation (DG), including energy storage, wind farm, and photovoltaic based on the power inverter. To ensure the stability of the MG, it is imminent for the engineers and scientists to design some reasonable control strategies. Please refer to the classical results on AC MG for details, such as (1–3).

For the AC MG, the hierarchical control method is well-used, i.e., the control is divided into the primary control, the secondary control, and the tertiary control. Specifically, the objective of the primary control is to design the droop control method such that the output voltage and frequency of DG track the corresponding reference signal (4). However, if only the droop control is used, then the deviation of the voltage and frequency will happen. To solve the problem, the secondary controller is usually introduced, which is implemented by introducing a consensus-based algorithm to regulate the voltage and frequency of their reference values. Finally, the tertiary control is to achieve optimal scheduling and economic indicators in a larger time range. This paper mainly focuses on the secondary control layer.

In general, the design methods of the secondary controller can be divided into the centralized control method and the distributed control method. The centralized one is to design the control method in a centralized manner (5–7), i.e., the controller of each DG needs the information of all DGs, which leads to this controller containing some disadvantages such as high computational complexity, high communication cost, and so on. To overcome those drawbacks, distributed secondary control method is proposed (8–11), where the

controller of each DG only needs the information from neighbor DGs, which contains the advantages of low communication cost and low computational complexity (12, 13).

Note that as the increase of the number of DGs in AC MG, system faults will inevitably occur, which may lead to the damage of the system performance (14). To ensure the reliability of the AC MG, some fault-tolerant secondary control methods have been developed. The existing fault-tolerant secondary control procedure can be divided into fault detection, fault estimation, and fault-tolerant, which is usually done in the above order. The wavelet analysis method as a fault detection method has been widely used to detect system faults. Based on the detection result, the fault estimation method and the fault-tolerant method will start work. In (16), a robust detector is designed to detect the consistency of measurements through the PMU measurements. In (17), a prototype method is developed to detect faults by using the candidate invariant to compare with the actual invariant. In (18), a vulnerability factor-based distributed fault detection method is proposed to detect the system faults. In addition, some results on fault-tolerant secondary control have been developed. In (19), a distributed fault-tolerant secondary controller is designed to achieve the frequency and voltage restoration by using the adaptive technique. In (20), a fault-tolerant cooperative secondary control scheme is developed for islanded MG with system faults by proposing a hidden layer.

Notice that the results mentioned above focus only on the fault detection or the fault-tolerant of the MGs separately. Besides, different from the faults on the inter-DG communication in MGs, the system faults on the secondary controller are usually more difficult to be detected and eliminated. Although some existing results have been developed to restore the voltage and frequency, the transient performance cannot be ensured and there are large fluctuations which are harmful to MG (22, 23). Based on the above observation, this paper considers the voltage and frequency regulation problems for AC MGs under the influence of faults. To solve this problem, the main method and the main contributions of this paper can be summarized as follows.

- To solve the reliability problem of AC MGs with system faults, a series of methods have been proposed, i.e., a wavelet analysis method is introduced to detect the system faults, the fault estimator is proposed to estimate the unknown faults, and the fault-tolerant controller is designed to eliminate the influence of faults.
- A k-step distributed fault estimator is proposed for each DG to estimate the fault signal. The main feature of this estimator is that with the increase of the number of k, the estimation error will be smaller and smaller until it converges to zero.
- Based on the developed k-step estimator, a distributed fault fault-tolerant secondary controller is designed to compensate for the influence of faults in AC MGs. Besides, the stability of the system is proved by the Lyapunov theorem.

The rest sections are organized as follows. In **Section 2**, the preliminaries are presented. In **Section 3**, the fault estimation design method is given. Then, a fault-tolerant controller is designed in **Section 4**. In **Section 5**, the simulation test is studied. Finally, the conclusion is given in **Section 6**.

2 Preliminaries

2.1 Graph theory

In this paper, the considered AC MGs is consisted of networks with DGs and leader nodes. The network topology is fixed and is defined by an undirected $\mathcal{G} = (\mathcal{W}, \mathcal{E}, \mathcal{A})$, where $\mathcal{W} = \{1, 2, \ldots, N\}$ represents the set of nodes, $\mathcal{E} \subset \mathcal{W} \times \mathcal{W}$ means the set of edges, and $\mathcal{A} = [a_{ij}]$ denotes the adjacency matrix. If there exists communication from i to node j, then the edge weight $a_{ij} = 1$; otherwise, $a_{ij} = a_{ji} = 0$. The in-degree matrix and the Laplacian matrix are denoted by $D = \text{diag}(d_1, \ldots, d_N)$ and $\mathcal{L} = D - \mathcal{A}$, where $d_i = \sum_{j=1}^{N} a_{ij}$.

Assumption 1. *The undirected network topology $\mathcal{G}$ is connected.*

2.2 System Model

In this paper, an AC MG is considered. It is assumed that the communication among DGs is ideal and the inductive distribution lines are considered. Besides, the active power and reactive power delivered by DG i at bus i satisfy

$$\begin{cases} P_i = \dfrac{v_{\text{bus},i} v_{\text{mag},i} \sin(\theta_i - \beta_i)}{Z_i}, \\[2mm] Q_i = -\dfrac{v_{\text{bus},i}^2}{Z_i} \dfrac{v_{\text{bus},i} v_{\text{mag},i} \cos(\theta_i - \beta_i)}{Z_i}, \end{cases} \quad (1)$$

where P_i and Q_i represent the active power and reactive power, respectively. $v_{\text{mag},i} \angle \theta_i$ and $v_{\text{bus},i} \angle \beta_i$ are the output voltage and bus voltage of DG i. Z_i represents the effective collective impedance of the output filter and the connector between distribution network and DG.

2.3 Control objective

The secondary control objective is to design secondary controllers of frequency and voltage regulation such that i) the frequency restores to its reference value ω_{ref} as frequency reference value; ii) the voltage regulates to $[v_{ref}^1, v_{ref}^2]$, where v_r^1 and v_{ref}^2 are the upper and lower bounds of voltage amplitude.

2.4 Cooperative control solution

Applying the droop control to (1), the following control scheme can be achieved

$$\begin{cases} \omega_i = \omega_{n_i} - n_{P_i} P_i, \\[2mm] v_{oi} = V_{n_i} - n_{Q_i} Q_i, \end{cases} \quad (2)$$

where ω_i represents the angular frequency. ω_{n_i} and V_{n_i} represent the set points in the secondary controller. n_{P_i} and n_{Q_i} represent droop coefficients chosen according to the power rating of the corresponding DG(17). By using an appropriate reference coordinate transformation, it is reasonable to adjust $v_{mag,i}$ by v_{oi}.

Driven by the consensus algorithm, the frequency error and voltage error among DGs are defined as follows.

$$e_{\omega,i} = c_\omega \left(\sum_{j\in\mathcal{N}_i} \left(\omega_j - \omega_i \right) + g_i \left(\omega_r - \omega_i \right) \right. \\ \left. + \sum_{j\in\mathcal{N}_i} \left(n_{P_j}P_j - n_{P_i}P_i \right) \right), \tag{3}$$

$$e_{v,i} = c_v \left(\sum_{j\in\mathcal{N}_i} \left(v_{oj} - v_{oi} \right) + g_i \left(v_r - v_{oi} \right) \right. \\ \left. + \sum_{j\in\mathcal{N}_i} \left(n_{Q_j}Q_j - n_{Q_i}Q_i \right) \right), \tag{4}$$

where ω_i and v_{oi} are the frequencies and output voltages of the DGs i-th DG. The positive constants c_ω and c_v are the coupling gains. ω_r and v_r are the frequency and voltage references, respectively.

Together with (2–4), it is shown that

$$e_{\omega,i} = c_\omega \left(\sum_{j\in\mathcal{N}_i} \left(\omega_{n_j} - \omega_{n_i} \right) + \sum_{\gamma=1}^{2} g_i \left(\omega_{n,\mathrm{ref}} - \omega_{n_i} \right) \right), \tag{5}$$

$$e_{v,i} = c_v \left(\sum_{j\in\mathcal{N}_i} \left(V_{n_j} - V_{n_i} \right) + \sum_{\gamma=1}^{2} g_i \left(V_{n,\mathrm{ref}}^\gamma - V_{n_i} \right) \right), \tag{6}$$

where $\omega_{n,\mathrm{ref}} = \omega_r + n_{P_i}P_i$ and $V_{n,\mathrm{ref}}^\gamma = v_{\mathrm{ref}}^\gamma + n_{Q_i}Q_i^1$.

To restore the frequency and voltage of all DGs to the reference values, ω_{ni} and V_{ni} are provided by the secondary controller, which are driven by the information from neighbors and updated according to the frequency and voltage error terms $e_{\omega,i}$ and $e_{v,i}$, respectively. From (2), we have

$$\begin{cases} \dot{\omega}_{ni} = \dot{\omega}_i + n_{P_i}\dot{P}_i = e_{\omega,i}, \\ \\ \dot{V}_{ni} = \dot{v}_{oi} + n_{Q_i}\dot{Q}_i = e_{v,i}. \end{cases} \tag{7}$$

Inspired by (21), we can design ω_{n_i} to stabilize ω_i and $n_{P_i}P_i$ and V_{n_i} to stabilize v_{oi} and $n_{Q_i}Q_i$. Combining (7) with (5, 6), the following distributed secondary controller can be designed

$$\dot{\omega}_{n_i} = c_\omega \left(\sum_{j\in\mathcal{N}_i} \left(\omega_{n_j} - \omega_{n_i} \right) + \sum_{\gamma=1}^{2} g_i \left(\omega_{n,\mathrm{ref}} - \omega_{n_i} \right) \right), \tag{8}$$

$$\dot{V}_{n_i} = c_v \left(\sum_{j\in\mathcal{N}_i} \left(V_{n_j} - V_{n_i} \right) + \sum_{\gamma=1}^{2} g_i \left(V_{n,\mathrm{ref}}^\gamma - V_{n_i} \right) \right). \tag{9}$$

Lemma 1. *Under Assumption 1, the designed distributed secondary controllers (8, 9) can regulate the frequency to its reference value and stabilize the voltage amplitude between the upper and lower bounds.*

---

1   The details of (5) and (6) are given in the Appendix.

3 Fault estimator design

3.1 Fault Model and analysis

Usually, faults may occur with the increase of system operation time in the secondary controller. In this paper, the fault signal is denoted by f_i, and the following conditions are satisfied.

Assumption 2. *The fault is changed slowly, i.e., the fault signal and its derivative are norm bounded as two positive scalars a and b ($\|f\| \le a$ and $\|\dot{f}\| \le b$).*

Under the influence of faults, the secondary controller of voltage regulation comes

$$\dot{V}_i = c_v \left(\sum_{j\in\mathcal{N}_i} \left(V_j - V_i \right) + \sum_{\gamma=1}^{2} g_i \left(V_r - V_i \right) \right) + f_i \\ = c_v \left(\sum_{\gamma=1}^{2} g_i V_r - \left(\left(d_i + \sum_{\gamma=1}^{2} g_i \right) V_i - \sum_{j\in\mathcal{N}_i} V_j \right) \right) + f_i. \tag{10}$$

Denote $V = [V_1,...,V_N]^T$, and $f = [f_1,...,f_N]^T$. Then, (10) can be rewritten as follows,

$$\dot{V} = c_v \left(G_1 \left(\mathbf{1}_N \otimes v_r \right) + G_2 \left(\mathbf{1}_N \otimes V_{\mathrm{ref}}^2 \right) \right. \\ \left. - \left(L + G_1 + G_2 \right) V \right) + f. \tag{11}$$

Define $\Theta_\gamma = \frac{1}{2}L + G_\gamma, \gamma = 1, 2$. Then, it has $L \left(\mathbf{1}_N \otimes V_{\mathrm{ref}}^\gamma \right) = (D - A) \left(\mathbf{1}_N \otimes V_{\mathrm{ref}}^\gamma \right) = 0, \forall \gamma = 1, 2$. Thus, (10) is rewritten as

$$\dot{V} = c_v \left(\left(\frac{1}{2}L + G_1 \right) \left(\mathbf{1}_N \otimes v_r \right) + \left(\frac{1}{2}L + G_2 \right) \right. \\ \times \left(\mathbf{1}_N \otimes V_{\mathrm{ref}}^2 \right) - \left(\frac{1}{2}L + G_1 + \frac{1}{2}L + G_2 \right) V \right) + f \\ = c_v \left(\sum_{\gamma=1}^{2} \Theta_\gamma \left(\mathbf{1}_N \otimes V_r \right) - \sum_{\gamma=1}^{2} \Theta_\gamma V \right) + f. \tag{12}$$

It can be seen that the normal secondary controller cannot achieve the voltage regulation objective under the influence of faults.

3.2 Fault estimators design

To estimate the voltage and fault of DG i, the following fault estimators can be designed.

$$\begin{cases} \dot{\hat{V}}_{i,0} = c_v \left(\sum_{j\in\mathcal{N}_i} \left(\hat{V}_{j,0} - \hat{V}_{i,0} \right) + g_i \left(V_r - \hat{V}_{i,0} \right) \right) + b_v \tilde{V}_{i,0} + \hat{f}_{i,0}, \\ \dot{\hat{f}}_{i,0} = -d_v \left(\sum_{j\in\mathcal{N}_i} \left(\tilde{V}_{j,0} - \tilde{V}_{i,0} \right) - g_i \tilde{V}_{i,0} \right), \end{cases} \tag{13}$$

where the positive constants b_v and d_v are coupling gains. $\hat{V}_{i,0}$ and $\hat{f}_{i,0}$ are the initial estimator states of DG i and $\tilde{V}_{i0} = V_i - \hat{V}_{i0}$ is the estimation error of V_i.

During the above estimator, the effect of fault-dependent term $\dot{f}$ is ignored, which may result in estimation bias. To eliminate this influence, the following k-step estimators are introduced.

$$\begin{cases} \dot{\hat{V}}_{i,k} = c_v \left(\sum_{j\in\mathcal{N}_i} \left(\hat{V}_{jk} - \hat{V}_{i,k} \right) + g_i \left(V_r - \hat{V}_{i,k} \right) \right) + b_v \tilde{V}_{i,k} + \hat{f}_{i,k}, \\ \dot{\hat{f}}_{i,k} = -d_v \left(\sum_{j\in\mathcal{N}_i} \left(\tilde{V}_{jk} - \tilde{V}_{i,k} \right) - g_i \tilde{V}_{i,k} \right) + \dot{\hat{f}}_{ik-1}, \end{cases} \tag{14}$$

where $\hat{V}_{i,k}$ and $\hat{f}_{i,k}$ are the k-step estimator states of DG i. $\tilde{V}_{i,k} = V_i - \hat{V}_{i,k}$ represents the estimation error.

Denote $\hat{V}_0 = [\hat{V}_{1,0}, \ldots, \hat{V}_{N,0}]$ and $\hat{f}_0 = [\hat{f}_{1,0}, \ldots, \hat{f}_{N,0}]$. The dynamics of (13) can be rewritten as,

$$
\begin{cases}
\dot{\hat{V}}_0 = c_\nu \left(\sum_{\gamma=1}^2 \Theta_\gamma (\mathbf{1}_N \otimes V_r) - \sum_{\gamma=1}^2 \Theta_\gamma \hat{V}_0 \right) + b_\nu \tilde{V}_0 + \hat{f}_0, \\
\dot{\hat{f}}_0 = d_\nu \sum_{\gamma=1}^2 \Theta_\gamma \tilde{V}_0.
\end{cases}
\tag{15}
$$

Define $\hat{V}_k = [\hat{V}_{1,k}, \ldots, \hat{V}_{N,k}]$ and $\hat{f}_k = [\hat{f}_{1,k}, \ldots, \hat{f}_{N,k}]$. The dynamic of (14) can be rewritten as

$$
\begin{cases}
\dot{\hat{V}}_k = c_\nu \left(\sum_{\gamma=1}^2 \Theta_\gamma (\mathbf{1}_N \otimes V_r) - \sum_{\gamma=1}^2 \Theta_\gamma \hat{V}_k \right) + b_\nu \tilde{V}_k + \hat{f}_k, \\
\dot{\hat{f}}_k = d_\nu \sum_{\gamma=1}^2 \Theta_\gamma \tilde{V}_k + \dot{\hat{f}}_{k-1}.
\end{cases}
\tag{16}
$$

Define $\tilde{f}_0 = f - \hat{f}_0$. From (15), it yields

$$
\begin{cases}
\dot{\tilde{V}}_0 = -\left(c_\nu \sum_{\gamma=1}^2 \Theta_\gamma + b_\nu \right) \tilde{V}_0 + \tilde{f}_0, \\
\dot{\tilde{f}}_0 = -d_\nu \sum_{\gamma=1}^2 \Theta_\gamma \tilde{V}_0 + \dot{f}.
\end{cases}
\tag{17}
$$

Define $\tilde{f}_k = f - \hat{f}_k$, for $k = 1, 2, \ldots$. It follows from (16) that

$$
\begin{cases}
\dot{\tilde{V}}_k = -\left(c_\nu \sum_{\gamma=1}^2 \Theta_\gamma + b_\nu \right) \tilde{V}_k + \tilde{f}_k, \\
\dot{\tilde{f}}_k = -d_\nu \sum_{\gamma=1}^2 \Theta_\gamma \tilde{V}_k + \dot{\tilde{f}}_{k-1}.
\end{cases}
\tag{18}
$$

From the above estimators, the following theorem can be achieved.

Theorem 1. *Under Assumptions 1 and 2, the proposed iterative estimators (13, 14) ensure that the estimation errors converge to zero as the iteration step k tends to ∞, i.e.,*

$$
\lim_{k \to \infty} \left(f - \frac{1}{k+1} \sum_{s=0}^k \hat{f}_s \right) = 0.
\tag{19}
$$

Proof. For $k = 0, 1, 2, \ldots,$ it follows from the estimation errors dynamics (17, 18) that

$$
\frac{\tilde{f}_k(t)}{k+1} = -d_\nu \int_0^t \sum_{\gamma=1}^2 \Theta_\gamma \frac{\sum_{s=0}^k \tilde{V}_s(\tau)}{k+1} d\tau + \frac{\int_0^t \dot{f}(\tau) d\tau}{k+1}.
\tag{20}
$$

According to the fact that $\sum_{\gamma=1}^2 \Theta_\gamma$ is a positive definite matrix and c_ν is a positive constant, it yields that the matrix $H = \begin{bmatrix} -\left(C_\nu \sum_{\gamma=1}^2 \Theta_\gamma + b_\nu \right) & I_N \\ -d_\nu \sum_{\gamma=1}^2 \Theta_\gamma & 0_N \end{bmatrix}$ is Hurwitz. Since $\dot{f}$ is bounded, then $\tilde{f}$ and $\tilde{V}$ are bounded, which implies that

$$
\lim_{k \to \infty} \frac{\tilde{f}_k(t)}{k+1} = 0.
\tag{21}
$$

Under Assumption 2, it is shown that f is bounded, which yields

$$
\lim_{k \to \infty} \frac{\int_0^t \dot{f}(\tau) d\tau}{k+1} = \lim_{k \to \infty} \frac{f(t) - f(0)}{k+1} = 0.
\tag{22}
$$

Together with (20–22), it yields

$$
\lim_{k \to \infty} \int_0^t \frac{1}{k+1} \sum_{s=0}^k \sum_{\gamma=1}^2 \Theta_\gamma \tilde{V}_s(\tau) d\tau = 0.
\tag{23}
$$

Then, it is shown that

$$
\lim_{k \to \infty} \frac{1}{k+1} \sum_{s=0}^k \sum_{\gamma=1}^2 \Theta_\gamma \tilde{V}_s = 0,
\tag{24}
$$

which implies that

$$
\lim_{k \to \infty} \frac{1}{k+1} \sum_{s=0}^k \tilde{V}_s = 0,
\tag{25}
$$

during which we have used the fact that $\sum_{\gamma=1}^2 \Theta_\gamma$ is positive definite. From $\tilde{V}_s = V - \hat{V}_s$, it follows that

$$
\lim_{k \to \infty} \sum_{s=0}^k \frac{1}{k+1} \left(V - \hat{V}_s \right) = 0.
\tag{26}
$$

Differentiate the equation as

$$
\lim_{k \to \infty} \sum_{i=1}^k \frac{1}{k+1} \left(\dot{V} - \dot{\hat{V}}_s \right) = 0.
\tag{27}
$$

According to (11, 15, 16), one has

$$
\lim_{k \to \infty} \frac{1}{k+1} \sum_{s=0}^k \left(-d_\nu \sum_{\gamma=1}^2 \Theta_\gamma \tilde{V}_s - b_\nu \tilde{V}_s - \hat{f}_s \right) + f = 0.
\tag{28}
$$

It further follows that

$$
\lim_{k \to \infty} \frac{1}{k+1} \sum_{s=0}^k \hat{f}_s = f.
\tag{29}
$$

$$
\lim_{k \to \infty} \frac{1}{k+1} \sum_{s=0}^k \tilde{f}_s = 0,
\tag{30}
$$

which implies that the mean value of $\tilde{f}_i$, $i = 0, 1, 2, \ldots, k$, can converge to zero when $k \to \infty$. □

4 Fault-tolerant controller design

In this section, a fault-tolerant controller is designed to recover the voltage to its reference value by compensating for the influence of unknown fault f_i. According to the conclusion in Theorem 1, we can define the estimation of the signal of fault as $f_{i,k}$, i.e.,

$$
f_{i,k} = \frac{1}{k+1} \sum_{s=0}^k \hat{f}_{i,s}.
\tag{31}
$$

Based on $f_{i,k}$, the following fault-tolerant controller V_i^d is designed,

$$
\dot{V}_i^d = \dot{V}_i - m_\nu f_{i,k}.
\tag{32}
$$

Define $V^d = [V_1^d, \ldots, V_N^d]^T$. Based on (31), the following dynamic can be achieved

$$
\dot{V}^d = \dot{V} - M_\nu F_k,
\tag{33}
$$

where $F_k = [f_{1k}, \ldots, f_{Nk}]^T$ and satisfies $F_k = \frac{1}{k+1} \sum_{s=0}^{k} \hat{f}_s$ according to (30).

Theorem 2. *If the condition in Theorem 1 is satisfied and the step k is large enough, then the controller designed based on iterative mean estimation information in* (31) *can ensure that the voltage restores to the normal value under the influence of faults.* **Proof.** Denote $\bar{V} = V^d - (\sum_{\gamma=1}^{2} \Theta_\gamma)^{-1} \sum_{\gamma=1}^{2} \Theta_\gamma (\mathbf{1}_N \otimes V_r)$. Under Assumption 1, we know that the matrix $\sum_{\gamma=1}^{2} \Theta_\gamma$ is non-singular and positive-definite. It follows from (32) that the derivative of $\bar{V}$ is

$$\dot{\bar{V}} = c_v \left(\sum_{\gamma=1}^{2} \Theta_\gamma (\mathbf{1}_N \otimes V_r) - \sum_{\gamma=1}^{2} \Theta_\gamma V \right) + f - F_k$$

$$= -c_v \sum_{\gamma=1}^{2} \Theta_\gamma \bar{V} + f - F_k. \tag{34}$$

Define $\bar{\Psi} = \Psi^T + \Psi$ and $\Psi = -c_v \sum_{\gamma=1}^{2} \Theta_\gamma$. Then, **formula (33)** can be rewritten as

$$\dot{\bar{V}} = \Psi \bar{V} + f - F_k. \tag{35}$$

Construct the Lyapunov function as $W = \bar{V}^T \bar{V}$. The time derivative of W along (34) is

$$\dot{W} = \bar{V}^T \bar{\Psi} \bar{V} + 2 \bar{V}^T (f - F_k). \tag{36}$$

Using Young's inequality leads to

$$2 \bar{V}^T (f - F_k) \leq \bar{V}^T \left(-\frac{1}{2} \bar{\Psi} \right) \bar{V} + (f - F_k)^T (-2\bar{\Psi}) (f - F_k)$$

$$\leq -\frac{1}{2} \bar{V}^T \bar{\Psi} \bar{V} + 2 \|\bar{\Psi}\| \cdot \|f - F_k\|^2. \tag{37}$$

TABLE 1 The AC MG parameters and the fault-tolerant controller parameters.

Lines impedance	$R_1 = R_3 = 0.5\Omega, R_2 = R_4 = 0.6\Omega$
Primary Controller	$m_i = n_i = 2e - 4$
Secondary Fault-Tolerant Controller	$c_{vi} = c_{wi} = 3, g_i^\gamma = 3$
Reference Signals	$w_{ref} = 50$ Hz, $v_{ref}^1 = 310$ V, $v_{ref}^2 = 311$ V
Load	$R_L = 2\Omega$

Substituting (36) into (35) yields

$$\dot{W} \leq \frac{1}{2} \bar{V}^T \bar{\Psi} \bar{V} + 2 \|\bar{\Psi}\| \cdot \|f - F_k\|^2. \tag{38}$$

From $\bar{\Psi} < 0$ and $f - F_k \to 0$ as $k \to \infty$, it shows that $\bar{V} \to 0$ as $k \to \infty$. Thus, it is shown that the voltage belongs to the set $[v_{ref}^1, v_{ref}^2]$. □

Remark 1. *Similarly, the developed can be also used to solve the frequency restore problem of MG under the influence of faults. Specifically, the frequency controller can be designed as follows,*

$$\begin{cases} \dot{\hat{\omega}}_{i,l} = c_\omega \left(\sum_{j \in \mathcal{N}_i} (\hat{\omega}_{j,l} - \hat{\omega}_{i,l}) + g_i (\omega_r^1 - \hat{\omega}_{i,il}) + g_i^2 (\omega_r^2 - \hat{\omega}_{i,l}) \right) + b_i \bar{\omega}_{i,l} + m_w \hat{f}_{i,l}, \\ \dot{\hat{f}}_{i,l} = -d_w \left(\sum_{j \in \mathcal{N}_i} (\tilde{\omega}_{j,l} - \tilde{\omega}_{i,l}) - \sum_{\gamma=1}^{2} g_i \tilde{\omega}_{i,l} \right) + \dot{\hat{f}}_{i,l-1}, \end{cases} \tag{39}$$

where $\dot{\hat{f}}_{i-1} = 0$. *The corresponding conclusions and stability analysis process are similar to that of voltage regulation and they are omitted here.*
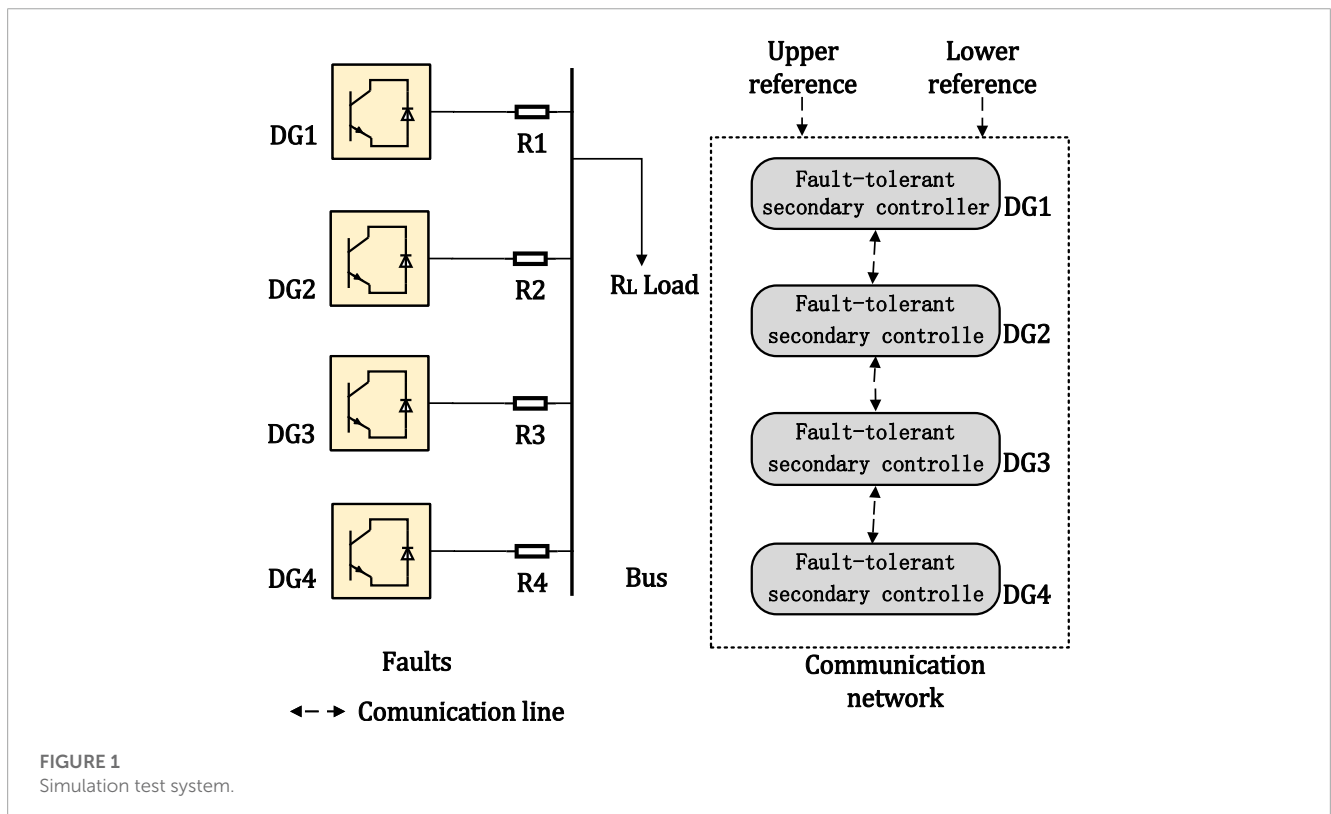

FIGURE 1
Simulation test system.

TABLE 2 The considered faults.

Time(s)	0–5	5–9	9–12	12–16
$f_{v,1}(t)$	0	5t	5t	5t
$f_{v,2}(t)$	0	0	40 sin t	40 sin t
$f_{v,3}(t)$	0	0	0	0
$f_{v,4}(t)$	0	0	0	40
$f_{w,1}(t)$	0	4t	4t	4t
$f_{w,2}(t)$	0	0	30 sin t	30 sin t
$f_{w,3}(t)$	0	0	0	0
$f_{w,4}(t)$	0	0	0	40

TABLE 3 Parameters of the designed fault-tolerant controller.

Fault-tolerant controller (31)	$b_v = 28, d_v = 13, m_v = 7$
Fault-tolerant controller (38)	$b_w = 22, d_w = 16, m_w = 8$
Iterative Number	$k = 6$

5 Simulation study

In this simulation, AC MG systems are considered, which consist of 4 DGs and 2 leaders as shown in **Figure 1**. The parameters of all DGs are shown in **Table 1**. To show the effectiveness of our developed fault-tolerant controller, the faults considered are displayed in **Table 2**, where $f_{v,i}$ and $f_{w,i}$ represent the attack signal on the voltage and frequency controller of DG i, respectively. Then, the following two cases are introduced to show the effectiveness of the developed method.

Case I. (Voltage and frequency regulation with distributed secondary controllers (Zhang et al., 2021) and (Anand et al., 2012)) In this case, the secondary controllers are added at $t = 2$ s. For the

secondary controllers (Zhang et al., 2021) and (Anand et al., 2012), the trajectories of voltage and frequency under faults are shown in **Figure 2**. The simulation result can be summarized from the following stages.

1) Stage 1 (0–2 s): Only primary control is actuated. The frequency ω_i is deviated from its reference value 50 Hz and the voltage V_i is also deviated from its reference range, i.e., [310,311].
2) Stage 2 (2–5 s): The secondary controllers (Zhang et al., 2021) and (Anand et al., 2012) are added at $t = 2$ s, which can restore the frequency ω_i to its reference value and can also control the voltage V_i to [310,311].
3) Stage 3 (5–9 s): The trajectories of frequency ω_1 deviate from its reference value and the trajectories of voltage V_1 cannot stay within its scope under faults signal $f_{v,1}$ and $f_{w,1}$ as shown in **Table 2**.
4) Stage 4 (9–12 s): The trajectories of frequency ω_1 and ω_2 deviate from its reference value and the trajectories of voltages V_1 and V_2 cannot stay within its scope with the addition of fault signals $f_{v,2}$ and $f_{w,2}$.
5) Stage 5 (12- s): All trajectories of frequency ω_i deviate from its reference value and the trajectories of voltage V_i cannot stay within its scope with the addition of fault signals $f_{v,2}$ and $f_{w,2}$.
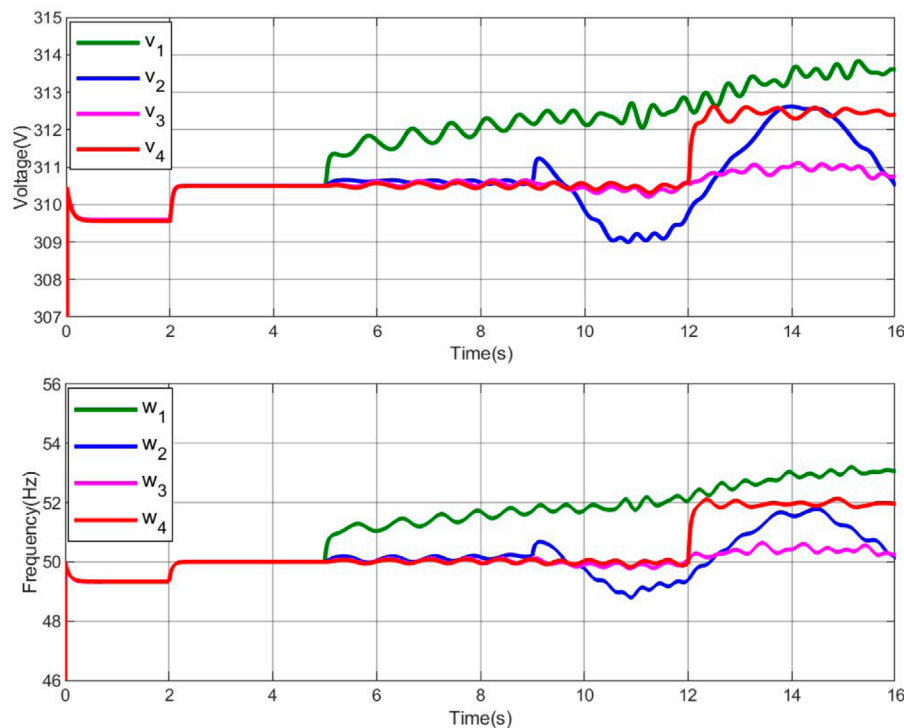

FIGURE 2
Trajectories of voltage and frequency with the distributed secondary controller (8)–(9) under faults.
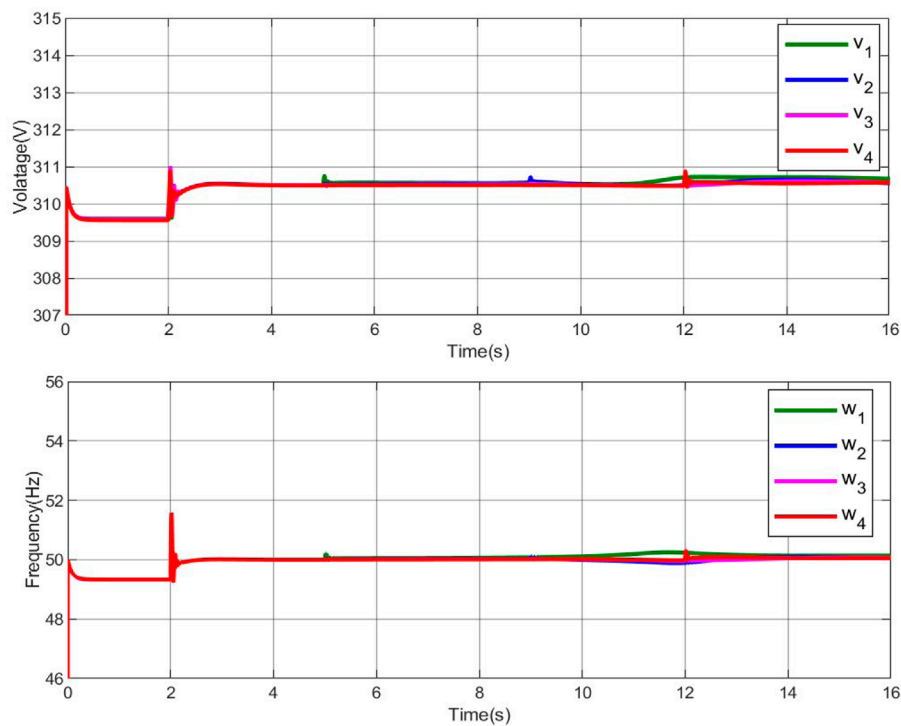
FIGURE 3
Trajectories of voltage and frequency with the secondary fault-tolerant controller (31) and (38) under faults.

In summary, under the distributed secondary controllers (Zhang et al., 2021) and (Anand et al., 2012)), the frequencies and voltages cannot be adjusted to the proper values under the influence of faults.

Case II. (Voltage and frequency regulation using distributed fault-tolerant controllers (31) and (38))

First, the parameters in the fault-tolerant controllers (31) and (38) are displayed in **Table 3**. Based on the distributed fault-tolerant controllers (31) and (38), the trajectories of voltage and frequency under the influence of faults are shown in **Figure 3**. Similar to case I, the following stages are shown.

1) Stage 1 (0–5 s): The conclusions are same to those in Stage 1 of Case I.
2) Stage 2 (5–16 s): The distributed fault-tolerant controllers (31) and (38) ensure that the frequency voltage are restored to their range.

Under the influence of the considered faults, the developed fault-tolerant control scheme can achieve the frequency recovery and voltage regulation effectively.

6 Conclusion

The distributed secondary fault-tolerant control problems of voltage and frequency regulation have been studied for smart grids under faults. A wavelet analysis and consensus algorithm-based fault-tolerant control method has been developed to solve the considered problems. In particular, the wavelet analysis technique is firstly introduced to detect the considered faults. Then, distributed secondary fault-tolerant controllers are designed to compensate for the influence of faults by using a newly introduced distributed fault estimate method. It is shown that the designed scheme ensures that both frequency regulation and voltage recovery objectives can be achieved. Finally, AC MGs with four distributed generations are used to validate the effectiveness of the developed fault-tolerant schemes.

Data availability statement

The original contributions presented in the study are included in the article/supplementary material, further inquiries can be directed to the corresponding author.

Author contributions

All the paper has been written by YH.

Funding

Conflict of interest

The authors declare that the research was conducted in the absence of any commercial or financial relationships that could be construed as a potential conflict of interest.

Publisher's note

All claims expressed in this article are solely those of the authors and do not necessarily represent those of their affiliated organizations, or those of the publisher, the editors and the reviewers. Any product that may be evaluated in this article, or claim that may be made by its manufacturer, is not guaranteed or endorsed by the publisher.

References

Anand, S., Fernandes, B., and Guerrero, J. (2012). Distributed control to ensure proportional load sharing and improve voltage regulation in low-voltage DC microgrids. *IEEE Trans. Power Electron.* 28 (4), 1900–1913. doi:10.1109/tpel.2012.2215055

Beg, O., Johnson, T., and Davoudi, A. (2017). Detection of false-data injection attacks in cyber-physical DC microgrids. *IEEE Trans. Ind. Inf.* 13 (5), 2693–2703. doi:10.1109/tii.2017.2656905

Bidram, A., and Davoudi, A. (2012). Hierarchical structure of microgrids control system. *IEEE Trans. Smart Grid* 3 (4), 1963–1976. doi:10.1109/tsg.2012.2197425

Chen, Y., Qi, D., Dong, H., Li, C., Li, Z., and Zhang, J. (2020). A FDI attack-resilient distributed secondary control strategy for islanded microgrids. *IEEE Trans. Smart Grid* 12 (3), 1929–1938. doi:10.1109/tsg.2020.3047949

Deng, C., WangWen, Y. C., Xu, Y., and Lin, P. (2020). Distributed resilient control for energy storage systems in cyber–physical microgrids. *IEEE Trans. Ind. Inf.* 17 (2), 1331–1341. doi:10.1109/tii.2020.2981549

Deng, C., Wen, C., Zou, Y., Wang, W., and Li, X. (2022). A hierarchical security control framework of nonlinear CPSs against DoS attacks with application to power sharing of AC microgrids. *IEEE Trans. Cybern.* 52 (6), 5255–5266. doi:10.1109/tcyb.2020.3029045

Ding, L., Han, Q., Ning, N., and Yue, D. (2019). Distributed resilient finite-time secondary control for heterogeneous battery energy storage systems under denial-of-service attacks. *IEEE Trans. Ind. Inf.* 16 (7), 4909–4919. doi:10.1109/tii.2019.2955739

Dou, C., Yue, D., and Guerrero, J. (2016). Multiagent system-based event-triggered hybrid controls for high-security hybrid energy generation systems. *IEEE Trans. Ind. Inf.* 13 (2), 584–594. doi:10.1109/tii.2016.2618754

Dragičević, T., Lu, X., Vasquez, J., and Guerrero, J. (2015). DC microgrids—Part I: A review of control strategies and stabilization techniques. *IEEE Trans. Power Electron.* 31 (7), 1–4891. doi:10.1109/tpel.2015.2478859

Fu, W., Ma, Q., Qin, J., and Kang, Y. (2021). Resilient consensus-based distributed optimization under deception attacks. *Int. J. Robust Nonlinear Control* 31 (6), 1803–1816. doi:10.1002/rnc.5026

Liu, Y., Ning, P., and Reiter, M. (2011). False data injection attacks against state estimation in electric power grids. *ACM Trans. Inf. Syst. Sec.* 14, 1–33. doi:10.1145/1952982.1952995

Lu, X., Guerrero, J., Sun, K., and Vasquez, J. (2013). An improved droop control method for DC microgrids based on low bandwidth communication with DC bus voltage restoration and enhanced current sharing accuracy. *IEEE Trans. Power Electron.* 29 (4), 1800–1812. doi:10.1109/tpel.2013.2266419

Mehrizi-Sani, A., and Iravani, R. (2012). Constrained potential function—based control of microgrids for improved dynamic performance. *IEEE Trans. Smart Grid* 3, 1885–1892. doi:10.1109/tsg.2012.2197424,

Modares, H., Kiumarsi, B., Lewis, F., Ferrese, F., and Davoudi, A. (2019). Resilient and robust synchronization of multiagent systems under attacks on sensors and actuators. *IEEE Trans. Cybern.* 50 (3), 1240–1250. doi:10.1109/tcyb.2019. 2903411

Morstyn, T., Hredzak, B., and Agelidis, V. (2016). Control strategies for microgrids with distributed energy storage systems: An overview. *IEEE Trans. Smart Grid* 9 (4), 3652–3666. doi:10.1109/tsg.2016.2637958

Ge, P., Chen, B., and Teng, F., " Event-triggered distributed model predictive control for resilient voltage control of an islanded microgrid," *Int. J. Robust Nonlinear Control*, 31, 2001, 1979, 2000. doi:10.1002/rnc.5238

Sahoo, S., Mishra, S., Peng, J., and Dragičević, T. (2018). A stealth cyber-attack detection strategy for DC microgrids. *IEEE Trans. Power Electron.* 34 (8), 8162–8174. doi:10.1109/tpel.2018.2879886

Sánchez, H., Rotondo, D., Escobet, T., Puig, V., and Quevedo, J. (2019). Bibliographical review on cyber attacks from a control oriented perspective. *Annu. Rev. Control* 48, 103–128. doi:10.1016/j.arcontrol.2019.08.002

Savaghebi, M., Jalilian, A., Vasquez, J., and Guerrero, J. (2012). Secondary control scheme for voltage unbalance compensation in an islanded droop-controlled microgrid. *IEEE Trans. Smart Grid* 3 (2), 797–807. doi:10.1109/tsg.2011. 2181432

Valenciaga, F., and Puleston, P. (2005). Supervisor control for a stand-alone hybrid generation system using wind and photovoltaic energy. *IEEE Trans. Energy Convers.* 20 (2), 398–405. doi:10.1109/tec.2005.845524

Wang, Z., and Passino, K. (2016). Stable reactive power balancing strategies of grid-connected photovoltaic inverter network. *Int. J. Robust Nonlinear Control* 26 (9), 2023–2046. doi:10.1002/rnc.3408

Zhang, H., Yue, D., Dou, C., Xie, X., Li, K., and Hancke, G. (2021). Resilient optimal defensive strategy of tSK fuzzy-model-based microgrids' system via a novel reinforcement learning approach. *IEEE Trans. Neural Netw. Learn. Syst.* doi:10.1109/TNNLS.2021.3105668

Zhao, J., Mili, L., and Wang, M. (2018). A generalized false data injection attacks against power system nonlinear state estimator and countermeasures. *IEEE Trans. Power Syst.* 33 (5), 4868–4877. doi:10.1109/tpwrs.2018.279 4468

Zhou, Q., Shahidehpour, M., Alabdulwahab, A., and Abusorrah, A. (2020). A cyber-attack resilient distributed control strategy in islanded microgrids. *IEEE Trans. Smart Grid* 11 (5), 3690–3701. doi:10.1109/tsg.2020. 2979160

Zuo, S., Beg, O., Lewis, F., and Davoudi, A. (2020). Resilient networked AC microgrids under unbounded cyber attacks. *IEEE Trans. Smart Grid* 11 (5), 3785–3794. doi:10.1109/tsg.2020.2984266